ARTICLE OPEN

Check for updates

Stellate ganglion block diminishes consolidation of conditioned fear memory in mice by inhibiting the locus coeruleus to the basolateral amygdala neural circuit

Ziheng Wang[1,2,3,7], Zhouliang Liu[3,4,5,7], Youjia Yu[6,7], Yuning Sun[1,2,3], Yan Zhang[1,3], Kailun Gao[1,3], Junli Cao[3,4,5]✉, Liwei Wang[1,2,3]✉ and Yangzi Zhu[2,3,5]✉

Posttraumatic stress disorder (PTSD) is a devastating, prevalent psychological disorder characterized by excessive fear memory because of exposure to severe trauma. Stellate ganglion block (SGB) is traditionally used as a clinical treatment for pain but has been regarded as an innovative therapy for PTSD in recent reports. However, the mechanisms underlying the effect of SGB on PTSD remain unknown. Here, we established a fear conditioning model, which is considered a representative model of traumatic memory, and evaluated the effect of SGB on conditioned fear memory. We found that SGB reduced conditioned fear memory in mice in conjunction with the hypoactivity of locus coeruleus (LC) noradrenergic and basolateral amygdala (BLA) glutamatergic neurons. The norepinephrine concentration in the BLA decreased after SGB. Moreover, conditioned fear memory was re-enforced when the LC NE (LC^{NE})-BLA pathway was activated in SGB mice. Our study findings indicated that the hypoactivity of the LC^{NE}-BLA pathway was the potential mechanism underlying the effects of SGB, which diminished consolidation of fear memory to relieve PTSD symptoms.

Translational Psychiatry (2025)15:172 ; https://doi.org/10.1038/s41398-025-03383-7

INTRODUCTION

Posttraumatic stress disorder (PTSD) is a psychiatric disorder that is widespread in individuals who have traumatic events and is characterized by excessive fear, anxiety and distress [1, 2]. Epidemiological study findings have suggested that the incidence of PTSD has increased in recent years [3]. A clinical study on PTSD showed that stellate ganglion block (SGB) treatments effectively ameliorated PTSD-related symptoms [4]. However, the neurobiological mechanisms of SGB in PTSD are still unknown. The stellate ganglion is a sympathetic ganglion located adjacent to the transverse process of seventh cervical that transmits sympathetic nerves to the heart, upper limbs and head [5, 6]. Previous studies have shown that there are anatomical connections from specific nuclei, such as the paraventricular nucleus of the hypothalamus and locus coeruleus (LC), in the central nervous system (CNS) to the stellate ganglion [7–9]. These anatomical connections allow SGB to regulate the function of the upstream nucleus to alleviate the stress response.

The stellate ganglion receives neural projections from the LC, which is located in the upper dorsolateral pontine tegmentum [10]. The LC is the largest group of noradrenergic (NE) cells in the whole brain, with diffuse NE output projections throughout the brain, and plays an essential role in a range of diverse physiological and pathological activities, particularly in arousal and stress [11–14]. Among the wide range of downstream regions that receive LC NE (LC^{NE}) projections, the basolateral amygdala (BLA) is critically involved in stress-induced emotional responses [15, 16]. The BLA is the prime subregion of the amygdala that integrates and processes emotional sensory information from cortical and subcortical regions, thus fulfilling its indispensable role in the fear memory consolidation process [16–19].

PTSD is characterized by the persistence of intense reactions to reminders of a traumatic event, altered mood, a sense of imminent threat, disturbed sleep, and hypervigilance [2]. Disorders involving excessive trauma-related fear and learning processes constitute one of the cores of PTSD pathology. In PTSD, fear memories continue to recur and tend to be vividly recalled as flashbacks when affected individuals exposed to trauma-like events, eventually leading to a fear cascade. The processing and regulation of fear is one of the key components of PTSD in both humans and rodents [2]. To mimic the core symptoms of PTSD in mice, it is not surprising that fear conditioning, in which rodents develop abnormally strong conditioned fear memories and react appropriately to threats, is widely adopted.

Therefore, we aimed to investigate whether SGB had effects on conditioned fear memory and, if so, what the potential underlying

[1]Department of Anesthesiology, Xuzhou Clinical College of Xuzhou Medical University, Xuzhou, Jiangsu, China. [2]Department of Anesthesiology, Xuzhou Central Hospital, Xuzhou, Jiangsu, China. [3]Jiangsu Province Key Laboratory of Anesthesiology, Xuzhou Medical University, Xuzhou, Jiangsu, China. [4]Jiangsu Province Key Laboratory of Anesthesia and Analgesia Application Technology, Xuzhou, Jiangsu, China. [5]NMPA Key Laboratory for Research and Evaluation of Narcotic and Psychotropic Drugs, Xuzhou Medical University, Xuzhou, Jiangsu, China. [6]Department of Anesthesiology, Suzhou Xiangcheng People's Hospital, Suzhou, Jiangsu, China. [7]These authors contributed equally: Ziheng Wang, Zhouliang Liu, Youjia Yu. ✉email: caojl0310@aliyun.com; doctorlww@sina.com; zhuyz@xzhmu.edu.cn

Received: 19 August 2024 Revised: 27 April 2025 Accepted: 7 May 2025
Published online: 17 May 2025

mechanisms are. Here, we hypothesized that the LC^{NE}-BLA pathway, a neural circuit critical for fear memory, is involved in the modulatory effect of SGB on conditioned fear memory. We explored the roles of LC^{NE} neurons, as well as the LC^{NE}-BLA pathway, in SGB in conditioned fear memory, providing a neural circuit basis for the clinical treatment of PTSD with SGB.

MATERIALS AND METHODS

Animals

Male C57BL/6J mice (8 weeks old) were obtained from Xuzhou Medical University (Xuzhou, Jiangsu Province, China) (SYXK 2016–0028). The mice were housed in groups and given *ad libitum* access to food pellets and water at constant humidity (55 ± 5%) and temperature (20 ± 2 °C) under a 12-h/12-h light/dark cycle (lights on 7 AM). All experimental procedures involving animals were approved by the Animal Care and Use Committee of Xuzhou Medical University.

Stellate ganglion block

All surgeries were performed under 2% sevoflurane anaesthesia. Mice were placed prone on an operating table with an insulation pad (37 °C). First, we palpated the left spinous process of the seventh cervical vertebra as an anatomical sign and moved a 1-mL syringe needle (Wuzhou Medical Equipment, Inc., Anhui, China) forwards along the left spinous process until the needle tip was beyond the vertebral body. The needle was then withdrawn 1 mm. Before injecting ropivacaine, we ensured that no blood or cerebrospinal fluid was present when the needle was retracted. Next, we injected 0.08 mL of 0.25% ropivacaine (Shunfen Pharmaceutical, Inc., Guangdong, China) into SGB group mice and 0.08 mL of normal saline (NS) (Shijiazhuang Fourth Pharmaceutical, Inc., Shijiazhuang, China) into NS group mice and stopped the administration of sevoflurane.

When the mice awakened from anaesthesia, we observed whether Horner syndrome (ptosis, miosis, and enophthalmos) appeared within 300 s on the block side [20]. The appearance of Horner syndrome was considered a sign of successful establishment of the SGB model; otherwise, SGB model establishment was considered unsuccessful, and we excluded these mice.

Fear conditioning

The fear conditioning experiment was conducted with a near-infrared video system (Med Associates Video Freeze Software, Med Associates, Inc., USA) consisting of two soundproof boxes, A and B, with different internal colours, that can block communication between mice inside and outside the boxes.

On Day 1, following a 90-s adaptation time, the mice were trained in box A, where they received three pairings of a tone (30 s, 2.2 kHz, 96 dB) (conditioned stimulus, CS) combined with a footshock (2 s, 0.7 mA) (unconditioned stimulus, US). Each CS/US pairing was separated by a 30-s intertrial interval. There was a 30-s free period after the final US, after which the mice were returned to their cages. After each training session, 75% ethanol was used to clean the box and eliminate odours.

On Day 2, following a 90-s adaptation time, the mice were tested in box B, where they received three tones without footshock. Each CS was separated by a 30-s intertone interval. The Med Associates Video Freeze System could recognize the freezing of the mice and record the freezing time automatically. There was a 30-s free period after the final CS, after which the mice were returned to their cages. After each test session, 75% ethanol was used to clean the box and eliminate odours.

Retrograde tracing of pseudorabies virus

We injected 1 μL of pseudorabies virus (PRV)-CAG-EGFP virus (BrainVTA, Inc., Wuhan, China) into the stellate ganglion under direct microscopic scrutiny. Five days later, the mice were anaesthetized with 10% chloral hydrate (0.1 ml/10 g, i.p.) (Puhuifen Chemical Technology, Inc., Shandong, China) and perfused transcardially with 20 mL of 0.9% saline followed by 30 mL of 4% paraformaldehyde (Vicmed Biotechnology, Inc., Xuzhou, China) in 0.1 M phosphate buffer (pH 7.4) (Vicmed Biotechnology, Inc.). The brain tissues were removed and postfixed in 4% paraformaldehyde overnight and cryoprotected in 30% sucrose. Thirty-micron-thick frozen sections from the brains of the mice were cut with a freezing microtome (Leica Biosystems, Wetzlar, German) and serially collected throughout the brain. Then, we observed EGFP expression in the whole brain under a confocal microscope (FV1000, Olympus Corp., Tokyo, Japan).

Stereotaxic surgery

All surgeries were performed under 2% sevoflurane anaesthesia. The mice were fixed in a stereotaxic frame equipped with a mouse adaptor (RWD Biotech Co., Shenzhen, China), and body temperature was maintained at 37 °C using a heating pad. After the skin was shaved and cut, the skull was wiped with H_2O_2 to identify the bregma and the lambda for head position adjustment. A cranial drill (RWD Biotech Co.) was used to open cranial windows for the implantation of guide cannulas, optical fibres or virus injection. For virus injection, the adeno-associated viruses (AAVs) (100–200 nL) were injected into the target areas (LC, AP: −5.45 mm, ML: ±1.00 mm, DV: −3.55 mm; BLA, AP: −1.24 mm, ML: ±3.24 mm, DV: −4.95 mm) via a Hamilton syringe with a blunted needle (Hamilton Company, Reno, NV, USA). The needle was allowed to remain in place for another 10 min after injection, ensuring the virus was well absorbed before retraction. Next, the scalp was sutured, and the animals were placed on a plate at 37 °C for recovery. The specific experimental strategies are detailed in the Supplementary Materials.

Immunofluorescence staining

The mice were anaesthetized with 10% chloral hydrate (0.1 mL/10 g, i.p.) and perfused transcardially with 20 mL of 0.9% saline followed by 30 mL of 4% paraformaldehyde in 0.1 M phosphate buffer (pH 7.4). The brain tissues were removed and postfixed in 4% paraformaldehyde overnight and cryoprotected in 30% sucrose. Thirty-micron-thick frozen sections from the mouse brains were cut using a freezing microtome and serially collected throughout the targeted region. Free-floating tissue sections were rinsed three times with PBS-T. The tissue sections were incubated with 10% normal donkey serum in PBS-T for 2 h, followed by incubation with the primary antibody at 4 °C for 24 h. After three 5-min rinses in PBS, the sections were incubated with secondary antibody in the dark for 2 h at 37 °C. The fluorescence intensity was visualized under a confocal microscope. Three to four sections per slide brain slice were collected bilaterally for each animal. The specific experimental strategies are detailed in the Supplementary Materials.

In vivo fibre-optic calcium imaging and neurotransmitter fluorescent probes for norepinephrine

A fibre photometry instrument (Inper Technologies, Hangzhou, China) was used to monitor and record GCaMP6s signals in LC^{NE} neurons. One week before the experiment was carried out, the mice were allowed to move freely on the experimenter's hand to adapt to the experimental environment and stimulus. Three weeks after virus injection, we monitored the fluorescent signals, which were equal to the signals of GCaMP6s in the LC, after the input section of the instrument was connected to the optical fibre. To assess the response of GCaMP6s in the LC to the CS, we defined the signal 3 s prior to stimulation as the baseline signal value (F0). We calculated the means of F0 and ΔF [(F–F0)/F0] for each point in the GCaMP6s trace, thus transforming the GCaMP6s signals into a ΔF trace diagram and heatmap. To measure the norepinephrine concentration, we used the NE2m probe, the second-generation GPCR-activation-based norepinephrine sensors with a superior response and high sensitivity and selectivity to norepinephrine in vivo. The experimental methods used for the norepinephrine probe were similar to those used for in vivo fibre-optic calcium imaging.

In vitro electrophysiology

Three weeks before fear conditioning training, the mice were injected with AAVs whose gene expression was under the control of the tetracycline responsive element (TRE) and Cre-dependent AAV (double loxP sites inverse of the AAV) to express TREs in BLA glutamatergic cells. When doxycycline (DOX) was present, the Tet-off system would be silent; otherwise, the Tet-off system would be activated. The mice were provided with water containing DOX (50 mg/kg) from the day of virus injection to two days before the training day. Then, the water containing DOX was removed to label the fear engram cells in fear conditioning. We identified fear engram (c-Fos-positive glutamatergic cells in fear conditioning) cells in the BLA via the Tet-off system.

The brain tissue was collected at 30 min after fear conditioning testing and placed in a cold high-sucrose solution for 5 min. The brain tissue containing the BLA region was cut into 300 μm slices with a vibratome. The slices were incubated in a high-sucrose slice mixture with 95% O_2 + 5% CO_2 and incubated in a 32 °C water bath for 30 min. Afterwards, the slices were transferred to artificial cerebrospinal fluid (ACSF).

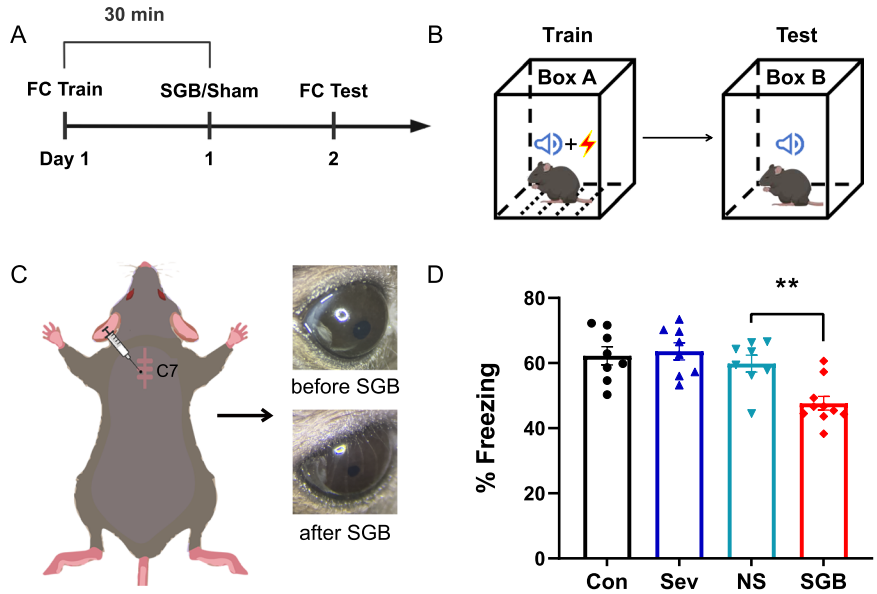

Fig. 1 Stellate ganglion block reduced conditioned fear memory. A Schematic of the behavioural experimental timeline. **B** The fear conditioning paradigm. **C** Schematic of stellate ganglion block (SGB) surgery and representative image of symptoms of SGB, indicating that the SGB model was established successfully. **D** SGB performed 30 min after fear conditioning training reduced conditioned fear memory [$n = 8$–10, F (3, 30) = 9.302, $P = 0.0002$; NS vs. SGB, $n = 8$–10, $P = 0.0074$], whereas anaesthesia alone or combined with normal saline (NS) did not affect conditioned fear memory [$n = 8$, F (2, 21) = 0.5132, $P = 0.6064$]. The data are presented as the mean ± standard error of the mean (SEM). $^{**}p < 0.01$.

We identified fear engram cells under a fluorescence microscope and recorded the spontaneous firing of these cells. The spontaneous firing frequency of neurons was recorded in I = 0 mode using a drawn glass microelectrode (7–12 M) near the BLA area (sealing resistance 80–120 M). For signal filtering and acquisition, a Multiclamp 700B patch clamp amplifier was used. Data were collected and analysed using a Digidata 1440 A digital-to-analogue converter and pClamp 10.2 software (Molecular Devices, LLC., San Jose, USA).

Chemogenetic and optogenetic manipulation

For chemogenetic manipulations, one week before the experiment was carried out, the mice were allowed to move freely on the experimenter's hand to adapt to the experimental environment and stimulus. Four weeks after virus injection, the mice received an intraperitoneal injection of clozapine N-oxide (CNO) (1 mg/kg, i.p.) (BrainVTA, Inc.) 30 min before the fear conditioning test to activate the LC^{NE}-BLA neural circuit. Then, we recorded the freezing time of the mice within the stimulus time window.

For optogenetic manipulations, 4 weeks after virus injection and fibre implantation, we used 473-nm laser generators (Inper Technologies) to generate blue light (473 nm, 20 Hz, 10 mW) to activate the terminals of BLA ChR2-transfected neurons. The blue light, delivered via the optical fibre implanted in the BLA, was turned on to examine the freezing time of the mice within the CS time window.

Drugs and drug delivery

Propranolol (10 mg/mL), CNO (1 mg/mL), kainic acid (KA) (2 mg/mL) and norepinephrine (2 mg/mL) were dissolved in sterile saline. Lidocaine (3%) and KA were infused bilaterally into the LC via delivery cannulas connected to the cannula drug delivery system in a 0.2 µL volume per side at a rate of 0.1 µL/10 s 30 min after training. Propranolol and norepinephrine were infused bilaterally into the BLA via delivery cannulas connected to the cannula drug delivery system in a 0.5 µL volume per side at a rate of 0.1 µL/10 s 30 min after training. All of the above drugs were obtained from MedChemExpress (MedChemExpress Biotechnology, NJ, USA).

Statistical analysis

If the virus injection or optical fibre implantation was not accurate, the animals or data points were excluded from the analysis. All the data were analysed with GraphPad Prism version 9 (GraphPad Software, Inc., California, USA). Group comparisons were performed via unpaired Student's t tests or one-way analysis of variance (ANOVA) with the Bonferroni multiple comparisons test. The statistical significance level was set at 0.05.

RESULTS

SGB reduced conditioned fear memory

We observed that the mice showed shorter freezing time after SGB, which indicated that SGB diminished conditioned fear memory in the mice. First, we established an SGB model in mice 30 min after fear conditioning training under inevitable sevoflurane anaesthesia. To exclude the effects of anaesthesia or volume injection on the behavioural performance of the mice, we evaluated the intensity of fear memory in the sevoflurane (Sevo) and normal saline (NS) groups. During the testing period, the duration of freezing in the SGB group was significantly shorter than that in the other three groups (Fig. 1D), and there were no significant differences in freezing time among the control (Con), Sevo and NS groups (Fig. 1D), indicating that anaesthesia alone or combined with NS did not affect fear memory. Our findings were consistent with those of previous studies.

To exclude the effect of SGB on locomotor activity in the mice, we measured the locomotor activity of the mice via the open field test (OFT) 24 h after training. There was no significant difference between the groups in total distance travelled (Fig. S2), indicating that SGB did not affect locomotor activity.

Additionally, to investigate the stage of memory affected by SGB, we performed different surgical procedures. Received SGB immediately or 30 min after training, the mice showed less freezing time during the testing period (Fig. 1D). When SGB was performed 6 or 24 h after training, the freezing time was not significantly different between the NS and SGB groups (Fig. S4). Mice that underwent SGB surgery 30 min after fear conditioning training presented a significant reduction in conditioned fear memory. Our data suggested that SGB diminished the consolidation of conditioned fear memory, which occurred within 2–6 h after fear conditioning training.

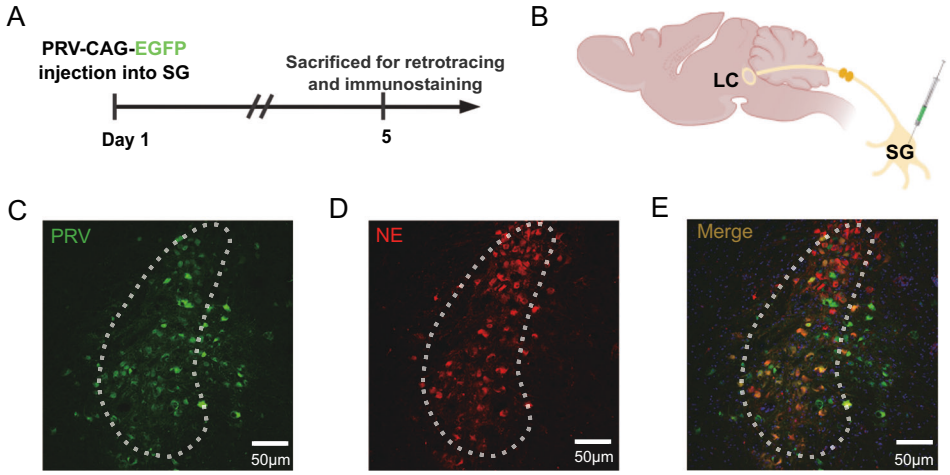

Fig. 2 The stellate ganglion received projections from the locus coeruleus. A, B Schematic of the pseudorabies virus (PRV) retrograde tracing experiment. **C** Representative images of PRV-expressing neurons in the locus coeruleus (LC); scale bar: 50 μm. **D** Representative fluorescence images of noradrenergic neurons in the LC; scale bar: 50 μm. **E** Representative images of PRV-expressing (green) and noradrenergic neurons (red) in the LC; scale bar: 50 μm.

Stellate ganglion received projections from the LC

To further explore the mechanisms underlying the effects of SGB on PTSD, we traced the connections from the CNS to the stellate ganglion by injecting PRV into the stellate ganglion (Fig. 2A, B). After 5 days, in the LC region as a whole, we observed significant EGFP expression, indicating that the stellate ganglion received projections from LC neurons (Fig. 2C). Immunofluorescence staining was used to identify the type of LC-projecting-stellate ganglion neurons (Fig. 2D). Immunofluorescence experiments showed that LC^{NE} neurons were costained with LC-projecting-stellate ganglion neurons (Fig. 2E). We identified the neural circuit from the brain to the peripheral ganglion, which is the pathway from LC^{NE} neurons to the stellate ganglion.

SGB inhibited the hyperactivity of LC^{NE} neurons

After identifying the neural circuit from the LC to the stellate ganglion, we determined whether fear conditioning altered the excitability of LC^{NE} neurons (Fig. 3A). We used a tyrosine hydroxylase (TH) antibody to identify NE neurons and assessed c-Fos expression levels, which equated with the excitability of LC^{NE} neurons (Fig. 3C). The percentage of c-Fos-positive neurons in the SGB group was lower than that in the NS group (Fig. 3B), indicating that SGB led to the hypoactivity of LC^{NE} neurons.

We also monitored the real-time calcium concentration to characterize the excitability of the LC^{NE} neurons during the test period via in vivo fibre-optic calcium imaging (Fig. 3D). Multiple trials in different animals consistently revealed a significant increase in response to the CS (Fig. 3E, F). The LC^{NE} neurons of SGB group mice showed lower excitability than those of NS group mice (Fig. 3G). This finding was consistent with the immunofluorescence results (Fig. 3B), and both findings led us to conclude that fear conditioning increased the excitability of LC^{NE} neurons and that SGB partially reversed this effect.

SGB inhibited the hyperactivity of BLA glutamatergic neurons

The BLA is the downstream region of the LC, which is essential for fear, and our retrograde tracing results confirmed the presence of the LC-BLA pathway (Fig. S5). Next, we assessed c-Fos expression levels in BLA glutamatergic neurons to characterize their excitability (Fig. 4A). We used the CaMKII antibody to identify glutamatergic neurons in the BLA. The percentage of costained neurons in the SGB group was lower than that in the NS group (Fig. 4B), indicating that SGB led to the hypoactivity of BLA glutamatergic neurons.

We also recorded the spontaneous firing frequency of BLA glutamatergic engram cells during fear conditioning to assess excitability at the single-cell level (Fig. 4D, E). The spontaneous firing frequency of engram glutamatergic neurons in the SGB group was significantly lower than that in the NS group (Fig. 4F). Both the immunofluorescence and electrophysiology results revealed the hypoactivity of BLA glutamatergic neurons after SGB, indicating that BLA glutamatergic neurons are involved in SGB.

SGB reduced the norepinephrine concentration in the BLA

The activation of LC^{NE} neurons drives diffuse norepinephrine release throughout branched axons. To better understand norepinephrine dynamics in the BLA in the fear context, we expressed NE2m to characterize the norepinephrine concentration in the BLA [21] (Fig. 5A). During fear conditioning testing, we observed a significant increase in NE2m fluorescence in both groups (Fig. 5B, C). However, SGB group mice showed lower concentrations of norepinephrine in the BLA than NS group mice (Fig. 5D). Our norepinephrine dynamics data suggested that SGB reduced conditioned fear memory, which was accompanied by a reduction in the norepinephrine concentration in the BLA.

SGB diminished consolidation of fear memory by inhibiting the LC^{NE}-BLA pathway

Clarifying the variations in excitability in both the LC and BLA regions, we attempted to manipulate the LC^{NE}-BLA pathway functionally to regulate conditioned fear memory in mice. First, we used chemogenetic techniques to manipulate the LC^{NE}-BLA pathway (Fig. 6A). During the test period, the NS+mCherry group presented longer freezing times than did the SGB+mCherry group (Fig. 6B). When chemogenetically activated, the SGB group showed significant increases in freezing time compared with the NS group (Fig. 6B). There was no significant difference between the NS+hM3D and NS+mCherry groups (Fig. 6B). Next, we optogenetically activated NS and SGB mice in the time window of the CS (Fig. 6C). During the CS, the freezing time of both ChR2 groups significantly increased (Fig. 6D). We observed increased freezing time in the SGB group compared with the NS group, and this increase was not significantly different from that in the NS

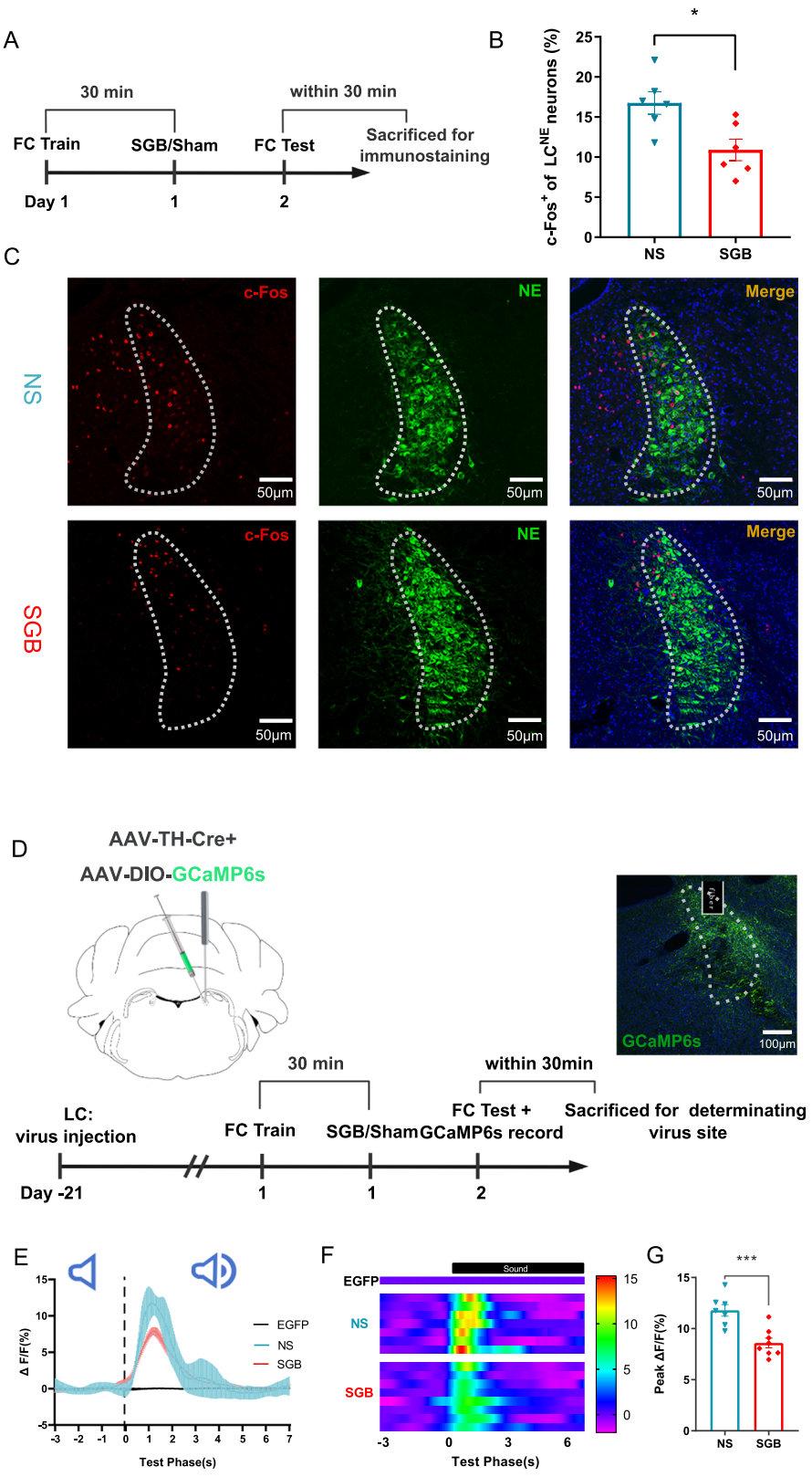

+ChR2 group (Fig. 6D). Our chemogenetic and optogenetic results suggested that the activation of the LC^{NE}-BLA neural circuit reversed the effect of SGB on conditioned fear memory and that SGB diminished consolidation of fear memory through the inhibition of the LC^{NE}-BLA pathway.

We also manipulated the LC and BLA functionally via pharmacological methods to regulate conditioned fear memory in mice. We injected lidocaine into the LC 30 min after training to temporarily block local neurotransmission and observed a significant reduction in fear memory (Fig. 6G). Pharmacological

Fig. 3 Stellate ganglion block inhibited the hyperactivity of locus coeruleus noradrenergic neurons. A Schematic of the immunofluorescence experimental timeline. **B** The expression of c-Fos in locus coeruleus noradrenergic neurons (LC^{NE}) neurons in the normal saline (NS) and stellate ganglion block (SGB) groups revealed that SGB led to the hypoactivity of LC^{NE} neurons (NS vs. SGB, $n = 6$, $t = 3.012$, $P = 0.0131$). **C** Representative images of c-Fos (red) in LC^{NE} (green) neurons; scale bar: 50 mm. **D** Schematic of the fibre-optic calcium imaging experimental timeline and representative images of GCaMP6s expression in the LC; scale bar: 100 μm. **E** Representative average per-stimulus line chart of fibre-optic calcium imaging in the test phase. **F** Representative average per-stimulus heatmap of fibre-optic calcium imaging in the test phase. **G** Representative summary data of the peak ΔF/F in the test phase revealed that SGB led to the hypoactivity of LC^{NE} neurons (NS vs. SGB, $n = 7–8$, $t = 4.963$, $P = 0.0003$). The data are presented as the mean ± standard error of the mean (SEM). $^{*}p < 0.05$, $^{***}p < 0.001$.

activation of the LC reversed the reduction in conditioned fear memory (Fig. 6G). Then, we injected the beta-adrenergic receptor blocker propranolol into the BLA to block the norepinephrine signal, which is derived mainly from the LC. We observed reduced freezing time in the NS+Prop group compared with NS+Vehicle group (Fig. 6H). The SGB-induced reduction in freezing time was reversed by norepinephrine injection (Fig. 6H). Pharmacological experiments on both regions repeatedly showed that SGB diminished fear memory consolidation by inhibiting the LC^{NE}-BLA pathway.

DISCUSSION

The major finding of our study was that SGB diminished consolidation of conditioned fear memory through inhibition of the LC^{NE}-BLA circuit. First, both immunofluorescence and in vivo fibre-optic calcium imaging revealed the hypoactivity of LC^{NE} neurons in SGB mice after the pathway of LC^{NE} neurons to the stellate ganglion was identified. Second, we found that SGB decreased the excitability of BLA glutamatergic neurons. Third, we observed that SGB reduced the norepinephrine concentration in the BLA. Finally, when the LC^{NE}-BLA circuit was chemogenetically and optogenetically activated, the mice presented stronger conditioned fear memory.

The memory process consists of complex periods: acquisition and encoding, consolidation, retrieval, and extinction [5]. In this study, we first established a fear conditioning mouse model, which is widely applied because of its remarkable resemblance to the conditioned fear behaviour of PTSD [15]. In the training phase of this model, the mice first undergo Pavlovian conditioning, in which an innocuous CS is paired with a nocuous US [22, 23]. In the testing phase, we evaluated the fear responses of the mice by their freezing time when the innocuous CS was presented alone. Fear conditioning in rodents effectively mimics the dysregulation of fear processes in PTSD patients in the clinical setting. We subsequently established the SGB model via minimally invasive percutaneous surgery [20], which is analogous to that performed in the clinical setting. Horner syndrome (ptosis, miosis, and enophthalmos), which is considered the typical symptom of SGB, was observed and recorded by a blinded experimenter [20, 24, 25]. We performed SGB at different time points—immediately, 30 min, 6 and 24 h after training—and set up a Sevo group to exclude the inevitable effects of anaesthesia. The behavioural results suggested that SGB had little effect on the retrieval of fear memory but diminished the consolidation of fear memory. The formation of fear memory is a time-dependent process in which unstable encoded information is consolidated into stable long-term memory within several hours [26, 27]. Once long-term memory is consolidated, extinguishing it is scarcely possible [28]. Our findings indicated that SGB decreased conditioned fear memory in mice by weakening its consolidation.

As reported in previous studies, SGB has been widely applied in the treatment of various psychological disorders, such as post-operative cognitive dysfunction, sleep disturbances and PTSD [4, 29–31]; however, the mechanisms underlying the effects of SGB remain unknown. A previous study showed that SGB attenuated stress responses accompanied by reduced blood concentrations of norepinephrine [32]. Norepinephrine, which is considered to play a critical role in cognitive processes such as stress, attention and learning, is a neurotransmitter that exists in both the CNS and peripheral nervous system [33, 34]. Notably, the presence of norepinephrine in the central or peripheral nervous system is independent because of the blood–brain barrier. The reduced norepinephrine concentration in the periphery of the SGB was verified, but we still did not observe a reduction in the norepinephrine concentration in the CNS. To study norepinephrine variations in the CNS, we confirmed transsynaptic projections from the LC to the stellate ganglion. The LC, which contains the largest group of NE neurons, is located at the bottom of the fourth ventricle, and the branched axons of these NE neurons extend throughout the CNS, such as to the hippocampus, neocortex, amygdala, cerebellum, thalamus, and spinal cord [35, 36]. The LC^{NE} system is reportedly associated with stress responses via the activation of β-adrenergic receptors in the BLA [37, 38]. Next, we labelled LC^{NE} neurons via immunofluorescence staining to define the cell types that project to the stellate ganglion. We identified the neural projections from LC^{NE} neurons to the stellate ganglion.

Catecholamines, including dopamine, epinephrine and norepinephrine, are neurotransmitters that are well known for their involvement in reward, emotion, addiction, and a range of cognitive behaviours [39]. Although the CNS neurotransmitter dopamine has received the most attention, norepinephrine is also crucial for a wide range of emotional and cognitive processes [40, 41]. An improvement in PTSD-related symptoms was observed when the norepinephrine concentration in the periphery was reduced. NE projections throughout the CNS are derived almost exclusively from the LC according to previous studies [9]. To understand whether LC^{NE} neurons respond to fear, we assessed c-Fos levels and calcium concentrations in LC^{NE} neurons [42]. Both experiments revealed that fear conditioning caused hyperactivity of LC^{NE} neurons. Memory consolidation is essential for the establishment of strong long-term memory, which involves the activation of many intracellular signalling pathways in specific neural networks [17, 43]. Reportedly, inactivation of the LC immediately after or 3 h after training induces memory deficit, and both behavioural and electrophysiological experiments have shown that the LC is widely engaged in multiple processes of memory, although the mechanisms remain incompletely understood [44]. We observed hypoactivity of LC^{NE} neurons after SGB surgery, which may be based on the projection of LCNE neurons to the stellate ganglion.

The BLA, which consists mainly of glutamatergic excitatory projection cells (80–85%) and gamma-aminobutyric acid interneurons (10–15%), is the downstream region of the LC [45, 46]. LC-derived norepinephrine signals induce long-term potentiation, which promotes encoding and consolidation of fear memory in BLA glutamatergic neurons [17]. Long-term potentiation at amygdala synapses, which involves complex signalling pathways, is essential for fear learning. Cyclic AMP response element-binding protein (CREB) is one of the representative protein elements and is shown to stimulate the induction of various immediate early gene transcription factors and some early effector genes [47]. These

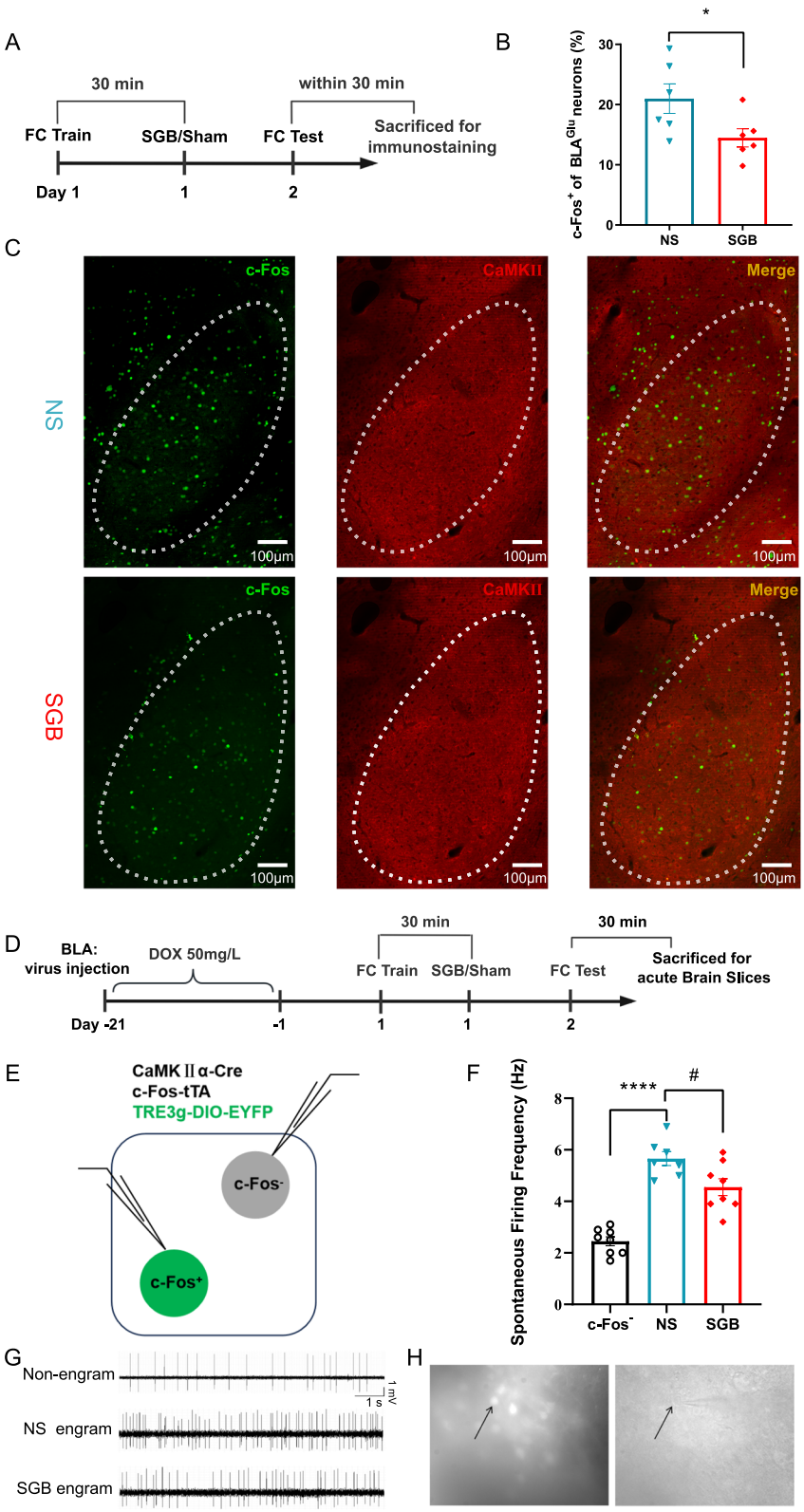

Fig. 4 Stellate ganglion block inhibited the hyperactivity of basolateral amygdala glutamatergic neurons. A Schematic of the immunofluorescence experimental timeline. **B** The expression of c-Fos in basolateral amygdala glutamatergic (BLA^{Glu}) neurons in the normal saline (NS) and stellate ganglion block (SGB) groups revealed that SGB led to the hypoactivity of BLA^{GLU} neurons (NS vs. SGB, $n = 6$, $t = 2.262$, $P = 0.0472$). **C** Representative images of c-Fos (green) in BLA^{Glu} (red) neurons; scale bar: 100 mm. **D** Schematic of the electrophysiology recordings timeline. **E** Schematic of the in vitro electrophysiology experimental timeline. **F** Spontaneous firing frequency of Non-engram and engram cells in the NS and SGB groups, which revealed that SGB led to the hypoactivity of BLA^{GLU} engram cells (NS vs. SGB, $n = 7$–8, $P = 0.0264$). **G** Diagram of spontaneous firing frequency in Non-engram and engram cells in the NS and SGB groups; scale bar: 1 mV, 1 s. **H** Schematic of recordings of engram cells. The data are presented as the mean ± standard error of the mean (SEM). $^{*}p < 0.05$, $^{\#}p < 0.05$, **** $p < 0.0001$.

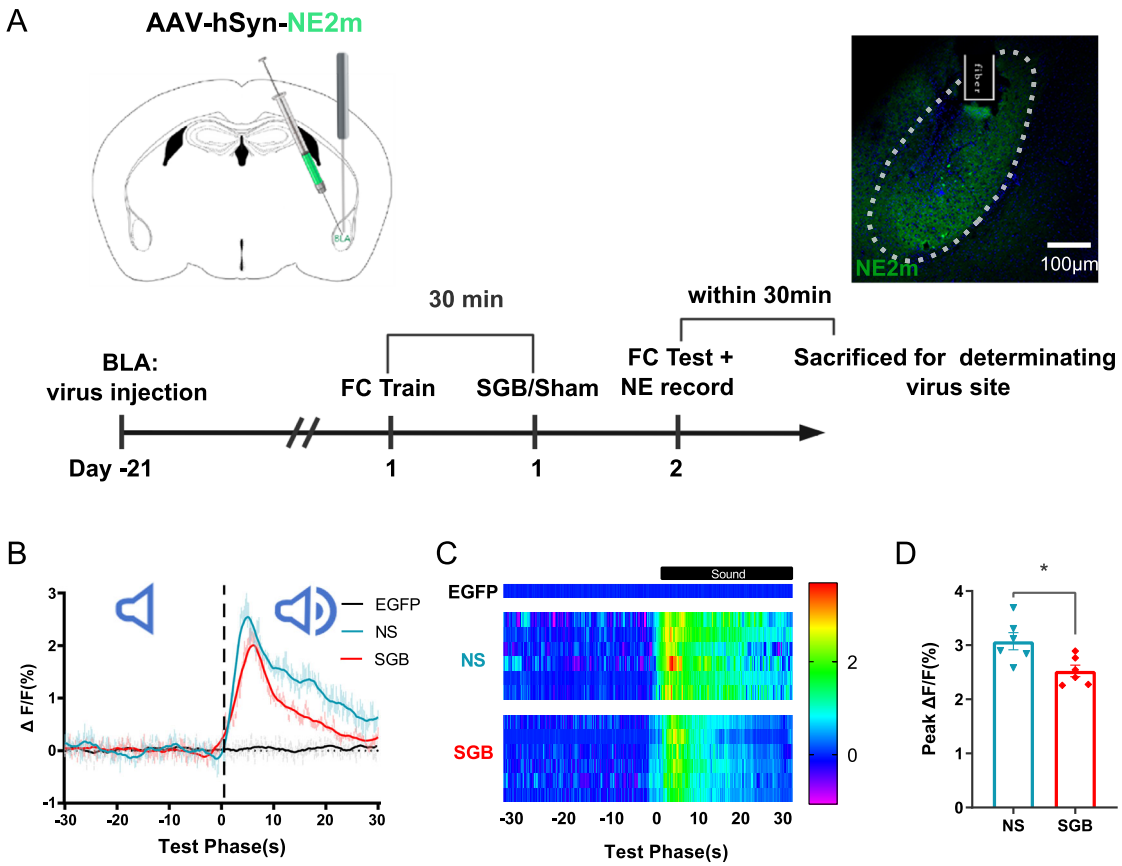

Fig. 5 Stellate ganglion block reduced the norepinephrine concentration in the basolateral amygdala. A Schematic of the experimental timeline for the measurement of norepinephrine concentrations and representative images of NE2m expression in the basolateral amygdala (BLA); scale bar: 100 μm. **B** Representative average per-stimulus line chart of norepinephrine fluorescence intensity in the test phase. **C** Representative average per-stimulus heatmap of norepinephrine fluorescence intensity in the test phase. **D** Representative summary data of the average ΔF/F in the test phase revealed that stellate ganglion block (SGB) reduced the norepinephrine concentration in the BLA (normal saline (NS) vs. SGB, $n = 6$, $t = 3.729$, $P = 0.0039$). The data are presented as the mean ± standard error of the mean (SEM). *$p < 0.05$.

initial transcriptional responses induce cascades of transcriptional events and genetic programs that cause adaptive modifications of synaptic transmission, such as long-term potentiation at the synapses of BLA glutamatergic neurons [47, 48]. In our study, we first assessed the excitability of BLA glutamatergic neurons as a whole and then recorded the spontaneous firing of BLA engram glutamatergic neurons at the single-cell level in vitro. We observed hypoactivity of BLA glutamatergic neurons in SGB mice, which indicated that SGB-induced alterations may occur predominantly in BLA glutamatergic neurons. In the BLA, we evaluated norepinephrine dynamics in vivo via NE2m, a genetically encoded fluorescent NE sensor that is based on the activation of the G protein-coupled receptor (GPCR). The NE signals in the BLA were highly increased but decreased in the mice that underwent SGB surgery. These results suggest that excessive fear memory is consistent with norepinephrine dynamics in the BLA and that norepinephrine is a crucial neurotransmitter that drives the encoding of conditioned fear memory.

All alterations occurring in the LC and BLA after SGB led us to focus on the LC^{NE}-BLA circuit. Previous studies have demonstrated that hyperactivity of the LC-BLA circuit leads to excessive anxiety and aversive memory, indicating the role of the LC-BLA circuit in processing emotional memory [49, 50]. To investigate the possible roles of the LC^{NE}-BLA circuit in SGB-induced attenuation of conditioned fear memory, we used chemogenetic and optogenetic techniques to activate the LC^{NE}-BLA circuit. The effect of SGB on conditioned fear memory was reversed when the LC^{NE}-BLA circuit of mice was activated chemogenetically and optogenetically. Strikingly, there was no robust enhancement of conditioned fear memory when the LC^{NE}-BLA circuit was activated, suggesting that fear conditioning resulted in strong activation of the LC^{NE}-BLA circuit. We also modulated the LC and BLA separately thorough pharmacological manipulations. Considering the extremely extensive efferent projections of the LC, it was not surprising that conditioned fear memory was dramatically affected when inhibition or excitation of the LC region as a whole occurred. Propranolol injection into the BLA reduced conditioned fear memory, and exogenous norepinephrine reversed the SGB-induced decreases in fear memory, suggesting that the SGB-induced reduction in conditioned fear memory was attributed to reduced norepinephrine concentrations in the BLA. On the basis of these results, we concluded that SGB diminished memory consolidation through inhibition of the LC^{NE}-BLA circuit.

There are several limitations and caveats that should be considered in this study. First, PTSD is a heterogeneous disorder with a multitude of symptoms, and fear conditioning mimics the dysregulation of fear memory, which is the core of PTSD development. However, different types of traumata may lead to differences in the subtypes of PTSD, and our findings should be confirmed in other models [51]. Second, we did not investigate the specific mechanisms by which LC-derived norepinephrine affects BLA neurons. Notably, different types of adrenoceptors in the BLA, such as beta and alpha-2 adrenoreceptors, which play opposing roles, have been reported [52]. Finally, our study focused

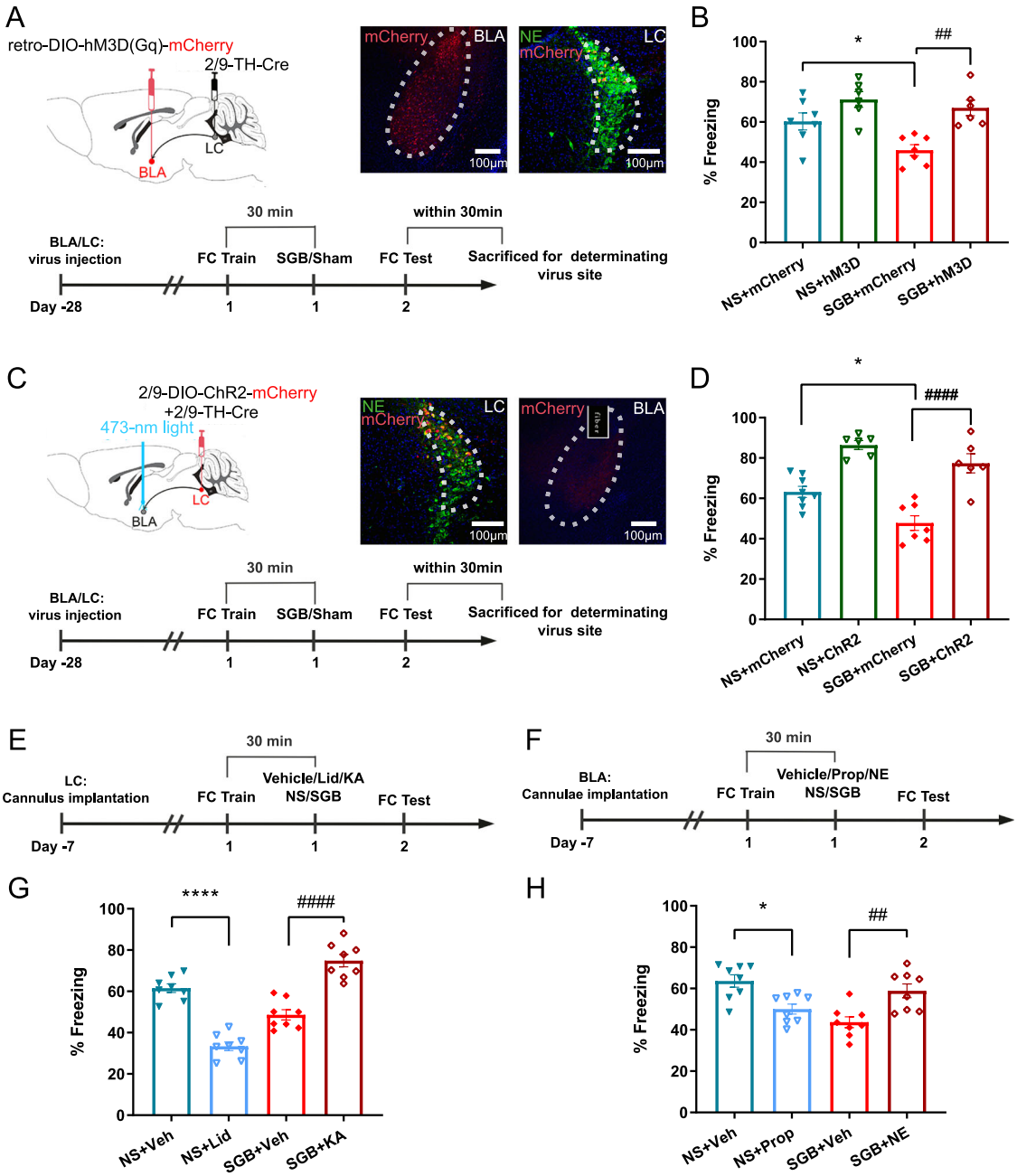

Fig. 6 Stellate ganglion block diminished fear memory consolidation by inhibiting the locus coeruleus noradrenergic–basolateral amygdala pathway. A Schematic of the chemogenetic experimental timeline and representative images of mCherry expression in the basolateral amygdala (BLA) and locus coeruleus (LC); scale bar: 100 μm. **B** Chemogenetic manipulations reversed the stellate ganglion block (SGB)-induced reduction in conditioned fear memory [$n = 6$–7, F (3, 22) = 8.999, $P = 0.0004$; NS + mCherry vs. SGB + mCherry, $n = 7$, $P = 0.0452$; SGB + mCherry vs. SGB + hM3D, $n = 6$–7, $P = 0.0037$; NS + mCherry vs. NS + hM3D, $n = 7$, $P = 0.2980$]. **C** Schematic of the optogenetic experimental timeline and representative images of mCherry expression in the BLA and LC; scale bar: 100 μm. **D** Optogenetic manipulations reversed the SGB-induced reduction in conditioned fear memory [$n = 6$–8, F (3, 23) = 23.81, $P < 0.0001$; NS + mCherry vs. NS + ChR2, $n = 6$–8, $P = 0.0004$; SGB + mCherry vs. SGB + ChR2, $n = 6$–7, $P < 0.0001$; NS + ChR2 vs. SGB + ChR2, $n = 6$, $P = 0.5436$]. **E** Schematic of the LC pharmacological manipulation experimental timeline. **F** Schematic of the timeline of BLA pharmacological manipulation experimental timeline. **G** Pharmacological inhibition of the LC reduced conditioned fear memory in mice, whereas activation of the LC reversed the SGB-induced reduction in conditioned fear memory [$n = 8$, F (3, 28) = 53.26, $P < 0.0001$; NS + Vehicle vs. NS + Lid, $n = 8$, $P < 0.0001$; SGB + Vehicle vs. SGB + KA, $n = 8$, $P < 0.0001$]. **H** Blocking beta receptors in the BLA reduced conditioned fear memory in mice, whereas activation in the BLA reversed the SGB-induced reduction in conditioned fear memory [$n = 8$, F (3, 28) = 9.713, $P < 0.0001$; NS + Vehicle vs. NS + Prop, $n = 8$, $P = 0.0134$; SGB + Vehicle vs. SGB + NE, $n = 8$, $P = 0.0049$]. The data are presented as the mean ± standard error of the mean (SEM). $^{*}p < 0.05$, $^{\#\#}p < 0.01$, $^{****}p < 0.0001$, $^{\#\#\#\#}p < 0.0001$.

mainly on BLA glutamatergic neurons, while GABAergic neurons in the BLA also play a crucial role [53]. Local plasticity of excitatory BLA neurons is thought to be critical for the establishment of conditioned fear memory; however, GABAergic neurons control the activity and plasticity of excitatory circuits in a spatial and temporal manner. Whether the SGB-induced reduction in fear memory involves the interaction of different subtypes of BLA neurons deserves further investigation.

In conclusion, we found that SGB diminished consolidation of conditioned fear memory in mice by inhibiting the LC^{NE}-BLA pathway, which plays an important role in fear memory consolidation. SGB induced a reduction in the norepinephrine concentration in the BLA, and regulation of the BLA norepinephrine concentration may be one strategy to prevent PTSD under certain conditions. In future studies, it will be important to further clarify the specific mechanisms underlying the effect of SGB on the LC^{NE}-BLA pathway to develop novel therapeutic strategies in clinical practice, ultimately leading to better prevention and treatment for people who have experienced traumatic events.

DATA AVAILABILITY

The data that support the findings of this study are available from the corresponding authors upon request.

REFERENCES

1. Herringa RJ. Trauma, PTSD, and the developing brain. Curr. Psychiatry Rep. 2017;19:69.
2. Maercker A, Cloitre M, Bachem R, Schlumpf YR, Khoury B, Hitchcock C, et al. Complex post-traumatic stress disorder. Lancet. 2022;400:60–72.
3. Dutheil F, Mondillon L, Navel V. PTSD as the second tsunami of the SARS-Cov-2 pandemic. Psychol. Med. 2021;51:1773–4.
4. Rae Olmsted KL, Bartoszek M, Mulvaney S, McLean B, Turabi A, Young R, et al. Effect of stellate ganglion block treatment on posttraumatic stress disorder symptoms: a randomized clinical trial. JAMA Psychiatry. 2020;77:130–8.
5. Kida S. Reconsolidation/destabilization, extinction and forgetting of fear memory as therapeutic targets for PTSD. Psychopharmacology. 2019;236:49–57.
6. Shi ZM, Jing JJ, Xue ZJ, Chen WJ, Tang YB, Chen DJ, et al. Stellate ganglion block ameliorated central post-stroke pain with comorbid anxiety and depression through inhibiting HIF-1α/NLRP3 signaling following thalamic hemorrhagic stroke. J. Neuroinflammation. 2023;20:82.
7. Jansen AS, Wessendorf MW, Loewy AD. Transneuronal labeling of CNS neuropeptide and monoamine neurons after pseudorabies virus injections into the stellate ganglion. Brain Res. 1995;683:1–24.
8. Krout KE, Mettenleiter TC, Loewy AD. Single CNS neurons link both central motor and cardiosympathetic systems: a double-virus tracing study. Neuroscience. 2003;118:853–66.
9. Jang I, Cho K, Moon S, Ko C, Lee B, Ko B, et al. A study on the central neural pathway of the heart, Nei-Kuan (EH-6) and Shen-Men (He-7) with neural tracer in rats. Am. J. Chin. Med. 2003;31:591–609.
10. Poe GR, Foote S, Eschenko O, Johansen JP, Bouret S, Aston-Jones G, et al. Locus coeruleus: a new look at the blue spot. Nat. Rev. Neurosci. 2020;21:644–59.
11. Maness EB, Burk JA, McKenna JT, Schiffino FL, Strecker RE, McCoy JG. Role of the locus coeruleus and basal forebrain in arousal and attention. Brain Res. Bull. 2022;188:47–58.
12. Breton-Provencher V, Sur M. Active control of arousal by a locus coeruleus GABAergic circuit. Nat. Neurosci. 2019;22:218–28.
13. Privitera M, von Ziegler LM, Floriou-Servou A, Duss SN, Zhang R, Waag R, et al. Noradrenaline release from the locus coeruleus shapes stress-induced hippocampal gene expression. Elife. 2024;12:RP88559.
14. McCall JG, Al-Hasani R, Siuda ER, Hong DY, Norris AJ, Ford CP, et al. CRH engagement of the locus coeruleus noradrenergic system mediates stress-induced anxiety. Neuron. 2015;87:605–20.
15. Izquierdo I, Furini CR, Myskiw JC. Fear memory. Physiol. Rev. 2016;96:695–750.
16. Llorca-Torralba M, Suárez-Pereira I, Bravo L, Camarena-Delgado C, Garcia-Partida JA, Mico JA, et al. Chemogenetic silencing of the locus coeruleus-basolateral amygdala pathway abolishes pain-induced anxiety and enhanced aversive learning in rats. Biol. Psychiatry. 2019;85:1021–35.
17. Zhang X, Kim J, Tonegawa S. Amygdala reward neurons form and store fear extinction memory. Neuron. 2020;105:1077–93.e7.
18. Zhang JY, Liu TH, He Y, Pan HQ, Zhang WH, Yin XP, et al. Chronic stress remodels synapses in an amygdala circuit-specific manner. Biol. Psychiatry. 2019;85:189–201.
19. Li M, Lv X, Li T, Cui C, Yang X, Peng X, et al. Basolateral amygdala cannabinoid CB1 receptor controls formation and elimination of social fear memory. ACS Chem. Neurosci. 2023;14:3674–85.
20. Duan Q, Zhou Y, Zhi J, Liu Q, Xu J, Yang D. Establishment of stellate ganglion block in mice. Eur. J. Med. Res. 2024;29:220.
21. Feng J, Zhang C, Lischinsky JE, Jing M, Zhou J, Wang H, et al. A genetically encoded fluorescent sensor for rapid and specific in vivo detection of norepinephrine. Neuron. 2019;102:745–61.e8.
22. Bienvenu TCM, Dejean C, Jercog D, Aouizerate B, Lemoine M, Herry C. The advent of fear conditioning as an animal model of post-traumatic stress disorder: learning from the past to shape the future of PTSD research. Neuron. 2021;109:2380–97.
23. Bouton ME, Maren S, McNally GP. Behavioral and neurobiological mechanisms of pavlovian and instrumental extinction learning. Physiol. Rev. 2021;101:611–81.
24. Abdi S, Yang Z. A novel technique for experimental stellate ganglion block in rats. Anesth. Analg. 2005;101:561–5.
25. Dellemijn PL, Fields HL, Allen RR, McKay WR, Rowbotham MC. The interpretation of pain relief and sensory changes following sympathetic blockade. Brain. 1994;117:1475–87.
26. Norris D. Short-term memory and long-term memory are still different. Psychol. Bull. 2017;143:992–1009.
27. Lee JLC, Nader K, Schiller D. An update on memory reconsolidation updating. Trends Cogn. Sci. 2017;21:531–45.
28. Grewe BF, Gründemann J, Kitch LJ, Lecoq JA, Parker JG, Marshall JD, et al. Neural ensemble dynamics underlying a long-term associative memory. Nature. 2017;543:670–5.
29. Yu K, Zhang XK, Xiong HC, Liang SS, Lu ZY, Wu YQ, et al. Stellate ganglion block alleviates postoperative cognitive dysfunction via inhibiting TLR4/NF-κB signaling pathway. Neurosci. Lett. 2023;807:137259.
30. Yang RZ, Li YZ, Liang M, Yu JJ, Chen ML, Qiu JJ, et al. Stellate ganglion block improves postoperative sleep quality and analgesia in patients with breast cancer: a randomized controlled trial. Pain. Ther. 2023;12:491–503.
31. Lipov E, Ritchie EC. A review of the use of stellate ganglion block in the treatment of PTSD. Curr. Psychiatry Rep. 2015;17:599.
32. Zhu G, Kang Z, Chen Y, Zeng J, Su C, Li S. Ultrasound-guided stellate ganglion block alleviates stress responses and promotes recovery of gastrointestinal function in patients. Dig. Liver Dis. 2021;53:581–6.
33. Joëls M, Fernandez G, Roozendaal B. Stress and emotional memory: a matter of timing. Trends Cogn. Sci. 2011;15:280–8.
34. Sanchez A, Toledo-Pinto EA, Menezes ML, Pereira OC. Changes in norepinephrine and epinephrine concentrations in adrenal gland of the rats submitted to acute immobilization stress. Pharmacol. Res. 2003;48:607–13.
35. Suárez-Pereira I, Llorca-Torralba M, Bravo L, Camarena-Delgado C, Soriano-Mas C, Berrocoso E. The role of the locus coeruleus in pain and associated stress-related disorders. Biol. Psychiatry. 2022;91:786–97.
36. Seo DO, Zhang ET, Piantadosi SC, Marcus DJ, Motard LE, Kan BK, et al. A locus coeruleus to dentate gyrus noradrenergic circuit modulates aversive contextual processing. Neuron. 2021;109:2116–30.e6.
37. Fukabori R, Iguchi Y, Kato S, Takahashi K, Eifuku S, Tsuji S, et al. Enhanced retrieval of taste associative memory by chemogenetic activation of locus coeruleus norepinephrine neurons. J. Neurosci. 2020;40:8367–85.
38. Chen FJ, Sara SJ. Locus coeruleus activation by foot shock or electrical stimulation inhibits amygdala neurons. Neuroscience. 2007;144:472–81.
39. Yuan L, Dou YN, Sun YG. Topography of reward and aversion encoding in the mesolimbic dopaminergic system. J. Neurosci. 2019;39:6472–81.
40. Isingrini E, Guinaudie C, Perret L, Guma E, Gorgievski V, Blum ID, et al. Behavioral and transcriptomic changes following brain-specific loss of noradrenergic transmission. Biomolecules. 2023;13:511.
41. Holland N, Robbins TW, Rowe JB. The role of noradrenaline in cognition and cognitive disorders. Brain. 2021;144:2243–56.
42. Dun NJ, Dun SL, Shen E, Tang H, Huang R, Chiu TH. c-fos expression as a marker of central cardiovascular neurons. Biol. Signals. 1995;4:117–23.
43. Terranova JI, Yokose J, Osanai H, Ogawa SK, Kitamura T. Systems consolidation induces multiple memory engrams for a flexible recall strategy in observational fear memory in male mice. Nat. Commun. 2023;14:3976.
44. Perez P, Chavret-Reculon E, Ravassard P, Bouret S. Using inhibitory DREADDs to silence LC neurons in monkeys. Brain Sci. 2022;12:206.
45. Ma LH, Li S, Jiao XH, Li ZY, Zhou Y, Zhou CR, et al. BLA-involved circuits in neuropsychiatric disorders. Ageing Res. Rev. 2024;99:102363.
46. Schmidt MV, Abraham WC, Maroun M, Stork O, Richter-Levin G. Stress-induced metaplasticity: from synapses to behavior. Neuroscience. 2013;250:112–20.
47. Santos TB, Kramer-Soares JC, Oliveira MGM. Contextual fear conditioning with a time interval induces CREB phosphorylation in the dorsal hippocampus and amygdala nuclei that depend on prelimbic cortex activity. Hippocampus. 2023;33:872–9.
48. Bocchio M, Nabavi S, Capogna M. Synaptic plasticity, engrams, and network oscillations in amygdala circuits for storage and retrieval of emotional memories. Neuron. 2017;94:731–43.
49. Giustino TF, Ramanathan KR, Totty MS, Miles OW, Maren S. Locus coeruleus norepinephrine drives stress-induced increases in basolateral amygdala firing and impairs extinction learning. J. Neurosci. 2020;40:907–16.
50. McCall JG, Siuda ER, Bhatti DL, Lawson LA, McElligott ZA, Stuber GD, et al. Locus coeruleus to basolateral amygdala noradrenergic projections promote anxiety-like behavior. Elife. 2017;6:e18247.

51. Richter-Levin G, Stork O, Schmidt MV. Animal models of PTSD: a challenge to be met. Mol. Psychiatry. 2019;24:1135–56.
52. Buffalari DM, Grace AA. Noradrenergic modulation of basolateral amygdala neuronal activity: opposing influences of alpha-2 and beta receptor activation. J. Neurosci. 2007;27:12358–66.
53. Skelly MJ, Ariwodola OJ, Weiner JL. Fear conditioning selectively disrupts noradrenergic facilitation of GABAergic inhibition in the basolateral amygdala. Neuropharmacology. 2017;113:231–40.

ACKNOWLEDGEMENTS

This study was supported in part by grants from the National Natural Science Foundation of China (NSFC82171912 to YZZ; NSFC82293641 to J-LC; NSFC82071903 to LWW); the National Key R&D Program of China—Sci-Tech Innovation 2030-Major Project (2021ZD0203100 to JLC) ;the Jiangsu Medical Key Discipline/Laboratory Construction Project (JSDW202231 to LWW) and the National Natural Science Youth Foundation (NSFC81801332 to YZZ).

AUTHOR CONTRIBUTIONS

YZZ, LWW and JLC initiated, designed and supervised the research. ZHW, ZLL, YJY, YNS and YZ performed the study and acquired data. ZHW, ZLL, YJY, and YZZ analyzed data. YZZ and ZHW wrote the manuscript. All authors read and approved the manuscript.

COMPETING INTERESTS

The authors declare no competing interests.

ETHICS APPROVAL AND CONSENT TO PARTICIPATE

This study involved only animal research. All experimental procedures involving animals were conducted with approved protocols from the Animal Care and Use Committee of Xuzhou Medical University (No. 202212S004).

ADDITIONAL INFORMATION

Supplementary information The online version contains supplementary material available at https://doi.org/10.1038/s41398-025-03383-7.

Correspondence and requests for materials should be addressed to Junli Cao, Liwei Wang or Yangzi Zhu.